Evaluation of Artificial Cranial Deformations on 3D Pre-Incas Mummified Skulls

Massimiliano Fantini[1], Francesca De Crescenzio[1], Franco Persiani[1],
Stefano Benazzi[2], Elena Tazzari[2], and Giorgio Gruppioni[2]

[1] Mechanical, Nuclear, Aviation, and Metallurgical Engineering – DIEM
University of Bologna
Bologna, Italy
[2] Histories and Methods for the Conservation of Cultural Heritage – DISMEC
University of Bologna
Bologna, Italy
massimiliano.fantini@unibo.it

Abstract

Pre-Columbian civilizations in South America used to induce artificial cranial deformations. Researchers in this field have studied modifications to skull morphology mainly by means of comparison of anthropometric indexes. In presence of mummified skulls, anthropologists are prevented from measuring the traditional osteometric landmarks due to the soft tissues that cover the reference points on the bones. In this paper, the study of a set of human mummified remains is presented. Three-dimensional (3D) models of four skulls, coming from Peru, are generated via Computed Tomography (CT). Reference landmarks have been selected and outline profiles have been identified on the virtual skulls in order to compute traditional anthropometric indexes. Finally, artificial cranial deformations have been evaluated combining 3D modeling with the results of previous scientific works.

1 Introduction

Artificial cranial deformation has been a very important practice in many cultures worldwide since the beginning of civilizations. Several populations applied this practice for different reasons, including political, religious or aesthetic. This practice was most popular and durable in regions of North and South America, where it has been performed into recent history.

Studying cranial and facial artificial shape modifications has always been a fundamental topic in the field of physical anthropology (McNeill and Newton 1965; Munizaga 1976; Allison et al. 1981; Rhode 2002; Friess and Baylac 2003; Tubbs et al. 2005). Valid scientific classification criteria are needed to estimate the place of origin and the cultural aspects of this practice. In the first systematic classification, Imbelloni (1930-31) reports two techniques that were used to induce deformations on the bones of the skull. The first technique used strings (annular deformation), while the second one used thin boards to tie the head in order to compress it (tabular deformation). If boards were located on the forehead and on the back of the head at different heights, they compressed the head so that the final shape was longer in the side view (*norma lateralis*) and larger in the front view (*norma frontalis*). Otherwise, the head was pushed on the cradle surface so that the back of the head was seriously flattened. Many authors deal with more detailed classifications based on geographical and ethnic characterizations (Allison et al. 1981; Gerszten 1993; Gerszten and Gerszten 1995; Rhode and Arriaza 2006).

Anthropologists need to establish whether a deformation was been induced on a skull by considering its morphological features. They take into account that boards and strings induce continuous and not discrete modifications of the shape. Most of the time, qualitative analyses based on the observation of the skulls are provided. In addition, morphometric indexes are computed in order to enforce the estimations about the presence and the type of deformations. This approach is normally applied to non-mummified skulls, providing quantitative information of linear and angular dimensions measured with contact-based instruments. For mummies, such measurements can not be taken on the actual remains due to the presence of soft tissue covering reference landmarks on the bones. Therefore, most of the previous studies on cranial deformation and the related information data set are focused on skulls.

Computed Tomography (CT) is a non-invasive technique applied to provide a digital representation of both the mummified surface and the skeletal structure (Hughes et al. 2005; Fantini et al. 2005; Winder et al. 2006). The most relevant advantage of this approach is the possibility of opening the way toward new concepts in morphometric reliefs that would not be possible on real remains. Hence, virtual models of bones extracted from mummies can be investigated in a virtual environment where anthropologists can use the conventional methods previously applied to real skulls. This approach allows researchers not only to preserve the skills and the knowledge related to the osteometric approach, but also to enhance the data collected in the past during excavation and physical anthropology investigations. Moreover, the virtual approach can dramatically reduce the effects of human errors in measuring, and such measurement can be repeated without disturbing the original remains.

The study described in this paper aims to reveal the presence and type of induced deformations on a set of four partially mummified skulls from Peru. It is based on porting the knowledge-based approach of previous works into a three-dimensional (3D) exploration of data. Reference landmarks

are selected and outline profiles are identified on the virtual skulls, properly oriented, in order to compute anthropometric indexes. Finally, cranial deformations are evaluated from quantitative and qualitative points of view, and a virtual model of the instruments (boards) used to induce such deformation is provided.

2 Materials and Methods

A set of four partially mummified skulls from the Civic Museums of Reggio Emilia has been analyzed in this work (Figure 1). The remains lack most of the archaeological context due to rough procedures performed during the excavations in the 19th century. The only information about these skulls is their Peruvian provenience, as neither the necropolis nor the exact time period from which they came are known. These facts limit the study on the cranial deformations of each skull since it depends on the regional and cultural context of such practices.

Nevertheless, since one of these skulls belongs to a mummy probably from the necropolis of Ancon, we consider the classification provided by Pardini, who collected dimensional data on a wide set of skulls from different necropoli in Peru (Ancon, Cuzco e Huache), and stored at the Anthropological Institute of the University of Florence.

Pardini (1970, 1971, 1974) proposed a classification system for cranial deformations according to the position of the boards used. He recognized that anterior-posterior tabular deformation was the most frequent practice in Pre-Columbian Peruvian period. At the same time, Imbelloni (1929) described artificial cranial deformation as erect tabular in the Ancon region. It is believed that in the Andean necropolis, compressing boards were positioned anteoposteriorly (both in the front and in the rear of the head), at different heights inducing particular shapes that Pardini defined as:

- Type I: inion-obelion;
- Type II: inion;
- Type III: lambda;
- Type IV: inion-lambda.

Moreover, Pardini, for each type of classification, created some reference silhouettes with the sketch of the boards positioned so as to induce the relative deformation (Figure 2)

Pardini characterized the skulls coming from the three necropolis of Ancon (Pardini 1970), Cuzco (Pardini 1974) and Huache (Pardini 1971) by means of the parameters reported in Table 1. Measurements have been taken according to standard osteometric landmarks and a method proposed by Martin and Saller (1958).

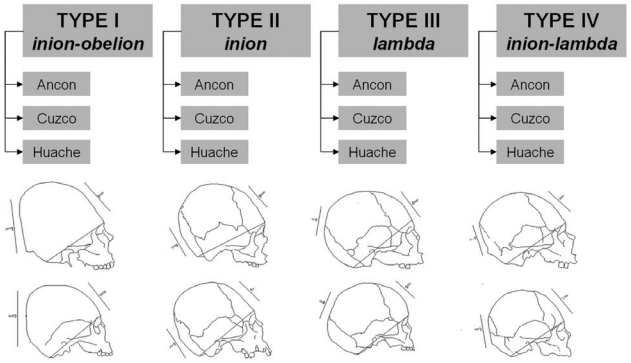

Figure 2. Artificial cranial deformations and boards position according to Pardini.

Table 1. Measurements used by Pardini with the reference numbers proposed by Martin and Saller (1958).

g-op	maximum head length	(1)
eu-eu	maximum head breadth	(8)
g-l	glabella-lambda length	(3)
br-ba	head height	(17)
ft-ft	minimal frontal breadth	(9)
co-co	maximum frontal breadth	(10)
anterior segment	glabella-lambda length in front of the basion-bregma segment	---
/br-l	bregma-lambda chord	(30)
)br-l	bregma- lambda arc	(27)
/l-i	lambda-inion chord	(31a)
)l-i	lambda-inion arc	(28a)
n-pr	upper facial height	(48)
zy-zy	maximum facial breadth	(45)
al-al	nose width	(54)
n-sn	nose height	(55)

Figure 1. Four partially mummified skulls from Peruvian necropolis.

3 3D Models Generation

3.1 CT Data Acquisition

In this project each mummified remain was examined with Computed Tomography (CT) performed by Philips Mx8000 Dual Scanner (Figure 3). The whole data-acquisition procedure was carried out by the radiology department of Faenza Hospital.

The CT scanning was performed at 1.5 mm slice intervals with a slice thickness of 6.5 mm for the main fragment of the mummy and at 1.3 mm slice intervals with a slice thickness of 1.3 mm for the three isolated mummified skulls. The image matrix had a resolution of 512 by 512 pixels and the number of axial slices resulting from CT of each acquisition can be found in Table 2. Finally, each CT data-set was stored as DICOM files.

Figure 3. Philips Mx8000 Dual CT Scanner.

Table 2. Number of axial slices resulting from CT acquisition of each sample.

Samples	Nr. of slices
Bust, head, left upper limb of the mummy (Skull 1)	267
Mummified Skull 2	153
Mummified Skull 3	152
Mummified Skull 4	154

3.2 Surface Reconstruction

A CT data set represents the radiopacity of the different tissues by grayscale intensity values; hard tissues, like bones, have high intensity while soft tissues, like skin, have lower intensity values. Therefore, both internal and external structures of mummified remains were reconstructed by setting different threshold values for each data set.

Starting from the stacks of CT slices, the digital 3D models of each skull (without mummified tissue) were built using Amira 3.1.1, an advanced software tool for 3D visualization, data analysis, and geometry reconstruction (Figure 4).

The models were achieved semi-automatically by threshold-based segmentation, contour extraction, and surface reconstruction. These features were particularly useful for distinguishing between the mummified tissue and the skeletal structure. Manual interventions, such as filling holes or deleting, erroneous polygon data were then performed in local regions to repair the models. Moreover, for the main fragment of the mummy (sample 1) a process for identifying and separating distinct bones was performed to isolate the model of the skull from the bust and the left upper limb.

The virtual 3D models (Figure 5) were rendered in order to observe the completeness and accuracy of the threshold and manual editing process. The list of the digital 3D models of each skull obtained with surface reconstruction of hard tissues is shown in Table 3 with the number of points and faces of the triangular mesh in the best resolution.

Next, specific anthropological analyses and measurements were conducted directly on the digital 3D models representing the hard tissues of the skulls. It is important to note that well defined landmarks on the surfaces of the bones are selectable only on these meshes, since the presence of soft

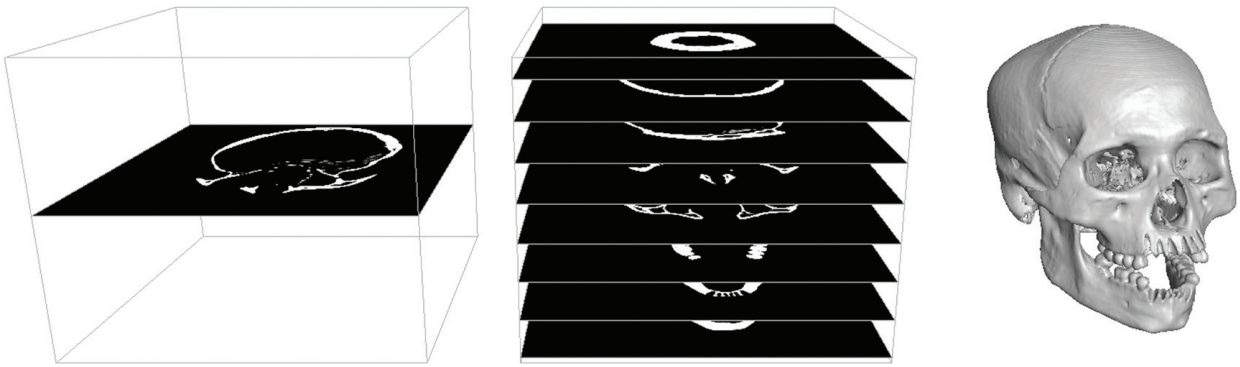

Figure 4. Single CT slice, stack loaded in bounding box and final model of the skull n. 4 resulting from the surface reconstruction process.

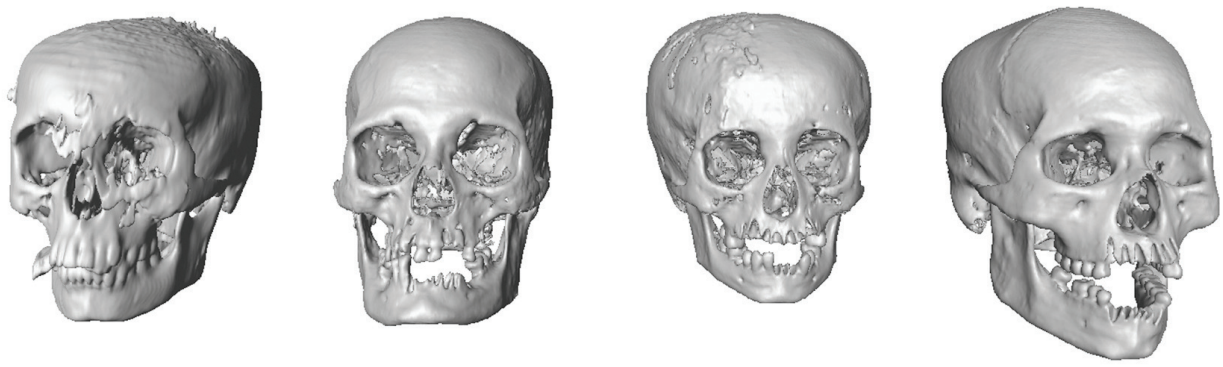

Figure 5. Virtual models of the skulls under investigation.

tissue prevents the same operations on the actual mummified remains.

4 Virtual Anthropology

4.1 3D Models orientation

The digital 3D models resulting from the previous step are not properly oriented since the orientation depends on the position of the samples during the CT data acquisition process. In order to insure repeatability and valid comparison of measurements, a detailed orientation procedure was applied by the integration of virtual reality and CAD (Computer Aided Design) tools leading to the computation of additional geometric features on the skulls.

First, the virtual skulls were oriented in a space of reference via the Frankfort Plane and the Mid-Sagittal Plane. The Frankfort Plane is the plane passing through three points of right and left porion and the lowest point in the left orbit. These points were manually identified on the virtual models by anthropologists and the correspondent Frankfort Plane was drafted (Figure 6).

Next, the Mid-Sagittal Plane, normal to Frankfort Plane, was identified. There is no standard method recognized about the points that define this plane. Hence, the normal plane to Frankfort Plane passing through glabella point and the midpoint of the line connecting right and left porion was chosen and drafted (Figure 7).

Table 3. Number of points and faces resulting from surface reconstruction process of hard tissues of each sample

Models	Nr. of points	Nr. of faces
Bust, head, left upper limb of the mummy (Skull 1)	1.205.034	401.678
Mummified Skull 2	1.459.320	486.440
Mummified Skull 3	1.433.802	477.934
Mummified Skull 4	1.473.570	491.190

4.2 Landmarks Identification

Anthropological measurements are based on a set of landmarks identified on the digital cranial surface. Bilateral landmarks were manually established on the virtual models per standard osteological landmark criteria (Martin and Saller 1958): mental foramen (ml), gonion (go), ectomolare (ecm), inferior zygion-maxillary point (zmi), alare (al), zygion (zy), lower inferior orbital point (or), ectoconchion (ek), maxillofrontale (mf), fronto-zigomatic (fmt), frontotemporal (ft), coronale (co), euryon (eu), stefanion (st). Next, in the same way, mid-sagittal landmarks were chosen on the section along the Mid-Sagittal Plane identified in the previous step: gnation (gn), pogonion (pg), infradentale (id),

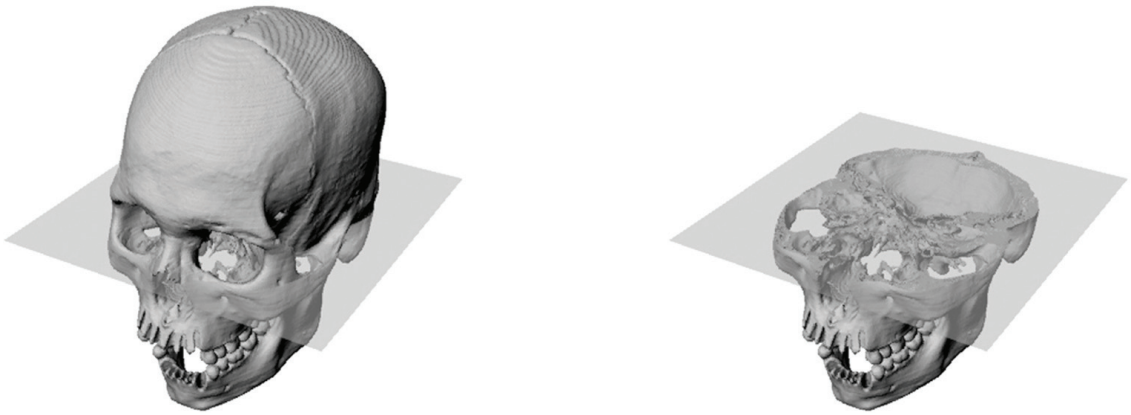

Figure 6. Identification of Frankfort Plane, passing through three points of right and left porion and left orbital.

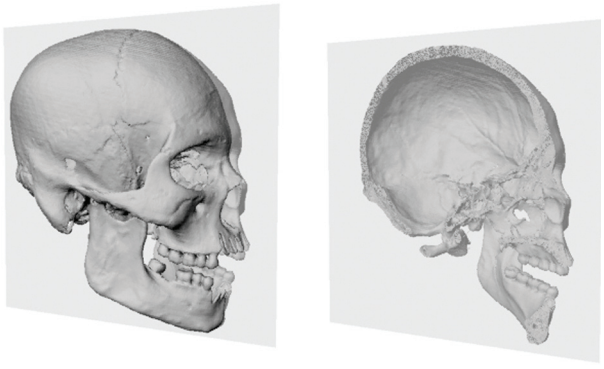

Figure 7. Identification of Frankfort Mid-Sagittal Plane, normal to Frankfort plane and passing through two points of glabella and midpoint of line between right and left porion.

prosthion (pr), staphilion (sta), subnasale (sn), nasion (n), glabella (g), bregma (br), vertex (v), obelion (ob), lambda (l), opistocranion (op), inion (i), opistion (o), basion (ba). Moreover, a set of angles used by Pardini to classify the artificial cranial deformations have been evaluated: Reicher angle, Falkenburger angle I, Falkenburger angle II, Klaatsch angle, Basion-opistion angle, Nasion-prostion angle (Figure 8).

With the set of identified landmarks, anthropometric indexes were evaluated and the results for each skull are shown in Table 4.

Table 4. Anthropometric indexes evaluated for each sample.

Parameters	Skull 1	Skull 2	Skull 3	Skull 4
Cranial index (8/1)	85.93	83.29	89.85	82.50
Cranial length- height index (17/1)	88.24	97.04	86.62	94.07
Cranial breadth- height index (17/8)	75.83	80.82	77.83	77.61
Medium-height Index (17/½(1+8))	81.56	88.19	81.99	85.05
Fronto-transv. I (9/10)	82.41	83.16	83.95	75.44
Anterior segment / 3	50.57	49.54	49.51	47.51
Parietal curvature index (30/27)	85.38	90.48	108.02	90.13
Occipital curvature index (31a/28a)	93.46	95.95	90.74	96.17
Reicher angle	130.71	128.41	132.52	116.05
Falkenburger angle I	90.93	88.31	87.26	90.06
Falkenburger angle II	0.57	0.53	8.70	5.96
Klaatsch angle	89.58	90.89	97.24	93.66
Basion-opistion angle	-5.30	-6.25	0.46	-6.18
Upper facial index (48/45)	49.13	47.84	49.84	47.41
Nasal index (54/55)	41.84	57.05	42.74	49.80
Nasion-prostion angle	85.69	82.01	91.02	79.27

5 Comparison

5.1 Multivariate analysis

With the aim of establishing a relationship between the statistical variables collected by Pardini and the measures taken on the mummified skulls, a multivariate analysis was performed (Squareform analysis of Standardized Euclidean distance, Jolliffe 2002). This procedure allows for collection of more statistical variables at a time, so we consider as a similitude index the minimum distance between the list of parameters taken on each of the four virtual skulls and the list computed by Pardini for each type analyzed (depicted in Table 5). This quantitative analysis shows how to connect data extracted from 3D models of mummies to statistical analyses made in previous works that contain an inestimable amount of data collected in the past. Nevertheless, it needs to be enforced by means of shape analysis procedures like the one described in the next section.

Each cell of Table 5 represents the Standardized Euclidean distance between

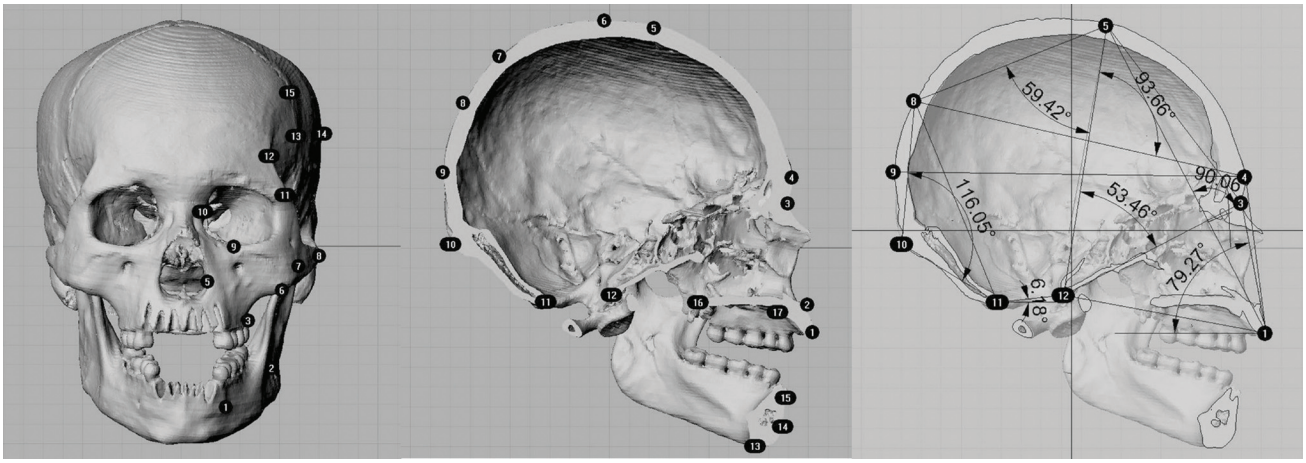

Figure 8. Identification of bilateral landmarks (left), mid-sagittal landmarks (center) and angles used by Pardini to classify the artificial cranial deformations (right).

Table 5. Squareform analysis of Standardized Euclidean distance.

		TYPE 1			TYPE 2			TYPE 3			TYPE 4		
		Ancon	**Cuzco**	**Huache**	**Ancon**	**Cuzco**	**Huache**	**Ancon**	**Cuzco**	**Huache**	**Ancon**	**Cuzco**	**Huache**
TYPE 1	**Ancon**	0,00	4,66	2,35	4,83	7,42	4,90	4,34	6,10	5,16	3,23	4,96	2,84
	Cuzco	4,66	0,00	5,73	6,64	5,13	7,30	4,97	5,92	5,94	5,47	4,16	5,24
	Huache	2,35	5,73	0,00	4,99	8,81	4,95	4,84	6,07	5,15	4,24	5,78	3,18
TYPE 2	**Ancon**	4,83	6,64	4,99	0,00	6,53	2,15	4,23	5,56	4,28	3,64	4,96	3,40
	Cuzco	7,42	5,13	8,81	6,53	0,00	7,42	6,01	6,91	6,66	6,41	4,88	6,85
	Huache	4,90	7,30	4,95	2,15	7,42	0,00	5,20	6,51	5,01	4,08	5,78	3,59
TYPE 3	**Ancon**	4,34	4,97	4,84	4,23	6,01	5,20	0,00	3,01	1,65	3,17	3,57	3,18
	Cuzco	6,10	5,92	6,07	5,56	6,91	6,51	3,01	0,00	2,75	5,28	3,86	5,07
	Huache	5,16	5,94	5,15	4,28	6,66	5,01	1,65	2,75	0,00	4,00	3,92	3,49
TYPE 4	**Ancon**	3,23	5,47	4,24	3,64	6,41	4,08	3,17	5,28	4,00	0,00	4,59	2,55
	Cuzco	4,96	4,16	5,78	4,96	4,88	5,78	3,57	3,86	3,92	4,59	0,00	4,06
	Huache	2,84	5,24	3,18	3,40	6,85	3,59	3,18	5,07	3,49	2,55	4,06	0,00
CASE STUDIES	**Skull 1**	5,15	6,79	5,75	4,95	7,07	5,81	4,04	5,54	4,88	4,26	6,15	5,08
	Skull 2	4,81	5,44	5,65	6,31	7,53	7,28	4,25	5,01	5,26	5,02	4,88	5,61
	Skull 3	8,08	9,47	8,49	5,98	8,64	6,97	7,62	7,83	7,83	6,73	7,29	7,25
	Skull 4	5,87	6,53	6,05	5,59	7,47	5,67	4,29	5,22	4,31	4,76	5,02	5,09

the statistical variables collected by Pardini and the measures taken on the mummified skulls so that the minimum distance for the four case studies (grey cells) allowed identifying the type of artificial cranial deformation induced:

Skull 1 – TYPE III (lambda) Ancon
Skull 2 – TYPE III (lambda) Ancon
Skull 3 – TYPE II (inion) Ancon
Skull 4 – TYPE III (lambda) Ancon

5.2 Silhouettes comparison

Besides the comparison between common lengths and indexes, the shapes of the skulls under investigation were compared with the relative reference skulls. Since Pardini provided more profiles for each type of deformation, such procedure were applied to each skull both for reference A and reference B belonging to the same type of deformation, as identified in previous step.

Silhouettes drafted by Pardini were scanned and transformed into vector format while silhouettes of the four skulls were extracted from the 3D models by means of the mid-sagittal section. Comparison between these silhouettes was focused on the rear semi-section identified by opistion-glabella segment (Figure 9).

Translation, rotation, and scale transformations were applied to the reference profiles in order to make them comparable with the extracted ones. The transformation procedure had three main steps. First, translation was applied overlaying the opistion of reference profile to the extracted one. Then, the reference profile was rotated around opistion to make the segments connecting glabella and opistion coincident on both profiles. Finally, the reference profile was scaled so that the two glabella points overlap on both profiles.

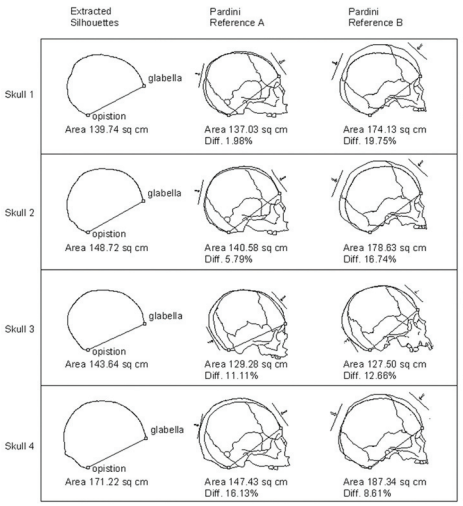

Figure 9. Area and difference calculation.

The difference between compared areas was measured in order to provide a quantitative similitude index and the position of boards, that induced the relative deformation, was extracted from the sketch of the reference skull minimizing the difference between areas.

Hence, according with Pardini, this procedure can suggest the correct position of boards used to induce the cranial deformation by observing the 2D drawings in Figure 9.

Finally, the sketches of the boards in their original position have been transformed into 3D models. Modeling and assembling the skull and the boards in 3D, the deformation process has been observed, studying the phenomenon as it really developed (Figure 10).

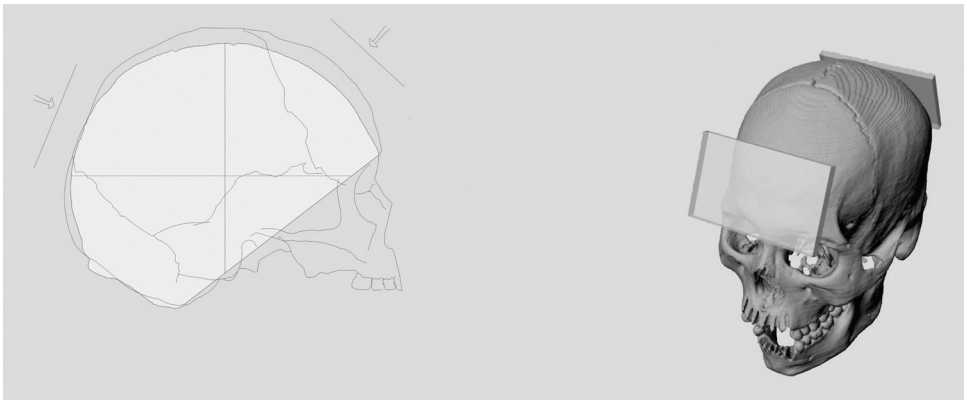

Figure 10. Silhouette comparison and visualization of compressing boards.

6 Conclusions

In this paper we presented a procedure to evaluate the artificial cranial deformations on a selected set of Peruvian mummified skulls by means of a virtual 3D approach. This approach is completely non invasive, based on the 3D virtual acquisition and analysis of the samples, and allows us to increase the amount of data collected from the skull. Unfortunately, few works in artificial cranial deformation analysis are based on data from a 3D approach, so the only way of comparing our results is taking into consideration those obtained in a traditional approach. Nevertheless, the different steps illustrated in this paper provide the opportunity to understand a new approach in detecting cranial deformation.

Statistical analyses highlighted the presence of cranial deformations belonging to the group classified as III (lambda artificial deformation) in the necropolis of Ancon for skull 1, skull 2 and skull 4. Instead, a type II deformation (inion) for skull 3 is obtained. Moreover, silhouette comparison allowed a 3D reproduction of the compression process. Due to the efficiency of 3D modeling, it is possible for people not trained in bio-archaeological reconstruction effectively to understand the locations of the boards used for skull deformation by advanced visualization systems.

Acknowledgements

Authors acknowledge Prof. Leonardo Seccia for his support in performing Multivariate Analyses.

References Cited

Allison, M., Gerszten, E., Munizaga, J., Santoro, C., and Focacci, G. 1981. La práctica de la deformación craneana entre los pueblos Andinos Precolombinos. *Chungara* 7:238-260.

Anton, S. C. 1989a. Facial structure: the influence of intentional vault deformation. *American Journal of Physical Anthropology* 78:184.

Anton, S. C. 1989b. Intentional cranial vault deformation and induced changes of the cranial base and face. *American Journal of Physical Anthropology* 79:253-267.

Cheverud, J. A. and Midkiff, J. E. 1992. Effects of fronto-occipital cranial reshaping on mandibular form. *American Journal of Physical Anthropology* 87:167-181.

Cheverud, L. A., Kohn, L. A. P., and Konigsberg, L. W. 1992. Effects of fronto-occipital artificial cranial vault modification on the cranial base and face. *American Journal of Physical Anthropology* 88:323–345.

Conlogue, G. 1999. Low kilovoltage, nonscreen mummy radiography. *Radiologic Technology* 71(2):125-32.

Conlogue, G., Forcier, D., Airo, M., Kilosky, J., Gambardella, S., Mansfield, K., and Greenwood, L. 1997. Radiographic evaluation of the soap man mummy. *Radiologic Technology* 68(5):391-8.

Fantini, M., Benazzi, S., De Crescenzio, F., Persiani, F., and Gruppioni, G. 2005. Virtual reconstruction of a dismembered Andean mummy from ct data. In, *VAST 2005. The 6th International Symposium on Virtual Reality, Archaeology and Intelligent Cultural Heritage: Short & Project Papers Proceedings*, M. Mudge, N. Ryan, R. Scopigno, eds., pp 61-66, 144. Pisa, Italy: CNR-ISTI.

Friess, M. and Baylac, M. 2003. Exploring artificial cranial deformation using elliptic Fourier analysis of Procrustes aligned outlines. *American Journal of Physical Anthropology* 122:11-22.

Hughes, S., Wright, R., and Barry, M. 2005. Virtual reconstruction and morphological analysis of the cranium of an ancient Egyptian mummy. *Australasian Physical & Engineering Sciences in Medicine* 28:122-127.

Imbelloni, J. 1930-31. I popoli deformatori delle Ande. La deformazione del cranio come arte e come elemento diagnostico delle culture. *Archivio per l'Antropologia e l'Etnologia* 60-61:90.

Jolliffe, I. T. 2002. Principal Component Analysis, Second Edition, Springer-Verlag, New York.

Kohn, L. A. P., Leigh, S. R., Jacobs, S. C., and Cheverud, J. M. 1993. Effects of annular cranial vault modification on the cranial base and face. *American Journal of Physical Anthropology* 90:147-168.

Gerszten, P. C. 1993. An investigation into the practice of cranial deformation among the pre-Columbian peoples of Northern Chile. *International Journal of Osteoarchaeology* 3:87-98.

Gerszten, P. C. and Gerszten, E. 1995. Intentional cranial deformation: a disappearing form of self-mutilation. *Neurosurgery* 37:374-381.

Martin, Rudolph and Saller, Karl. 1958. *Lehrbuch der Anthropologie*. Stuttgart: Gustav Fischer Verlag.

McNeill, R. W. and Newton, G. N. 1965. Cranial base morphology in association with intentional cranial vault deformation. *American Journal of Physical Anthropology* 23:241-254.

Munizaga, J. R. 1976. Intentional cranial deformation in the pre-Columbian populations of Ecuador. *American Journal of Physical Anthropology* 45:687-694.

Pardini, E. 1970. I calvari della necropoli di Ancon. *Archivio per l'Antropologia e l'Etnologia* 100:29.

Pardini, E. 1971. I calvari della Huache di Lima. *Archivio per l'Antropologia e l'Etnologia* 101:105.

Pardini, E. 1974. I calvari del Cuzco. *Archivio per l'Antropologia e l'Etnologia* 104:113.

Rhode, M. P. 2002. Cranial deformation and measurement stability among prehistoric South Central Andean populations [abstract]. *American Journal of Physical Anthropology* [Suppl] 117(S32):30.

Rhode, M. P. and Arriaza, B. T. 2006. Influence of cranial deformation on facial morphology among prehistoric south central Andean populations. *American Journal of Physical Anthropology* 130:462-470.

Schijman, E. 2005. Artificial cranial deformation in newborns in the pre-Columbian Andes. *Child's Nervous System* 21: 945-950.

Tubbs, R. S., Salter, E. G., and Oakes, W. J. 2006. Artificial deformation of the human skull: a review. *Clinical anatomy* 19(4):372-7.

Winder, R. J., Glover, W., Golz, T., Wulf, J., McClure, S., Cairns, H., and Elliott, M. 2006. "Virtual unwrapping" of a mummified hand. *Studies in Health Technology and Informatics* 119:577-82.